CHAPTER

17

Cable Properties and Information Processing in Dendrites

Michael Beierlein

Neurons form elaborate extensions termed dendrites that receive and integrate a myriad of inhibitory and excitatory synaptic inputs. The overall size and branching pattern can differ dramatically between different neuronal types (Fig. 17.1) suggesting that dendritic trees are critical for the computational tasks carried out by a given neuron. One of the main challenges in modern neuroscience is to understand how the properties of dendritic trees shape information-processing functions in individual neurons. An important step toward this goal is to reveal how different parts of a neuron interact.

Neurons carry out five basic functions (Fig. 17.2):

1. Generate intrinsic activity (at any given site in the neuron through voltage-dependent membrane properties and internal second-messenger mechanisms).
2. Receive synaptic inputs (mostly in dendrites, to some extent in cell bodies, and in some cases in axon hillocks, axon initial segments and axon terminals).
3. Integrate signals by combining synaptic responses with intrinsic membrane activity (in dendrites, cell bodies, axon hillocks and axon initial segments).
4. Encode output patterns in graded potentials or action potentials (at any given site in the neuron).
5. Distribute synaptic outputs (from axon terminals and, in some cases, from dendrites).

This chapter will first outline a quantitative description of the passive electrical properties of dendritic trees, which influence synaptic integration. We will then consider the properties of active dendrites and their role in more complex types of information processing.

BASIC TOOLS: CABLE THEORY AND COMPARTMENTAL MODELS

The electrotonic properties of neurons that underlie the spread of electrical current are often referred to as *cable properties*. Electrotonic theory was first applied mathematically to the nervous system in the late 19th century for spread of electric current through nerve fibers. By the 1930s and 1940s, it was applied to simple invertebrate axons—the first steps toward the development of the Hodgkin–Huxley equations (Chapters 12 and 14) for the action potential in the axon.

Mathematically, it is impractical to apply cable theory to branching dendrites, but in the 1960s Wilfrid Rall showed how this problem could be solved by the development of computational compartmental models (Rall, 1964; Rall, 1967; Rall, 1977; Rall and Shepherd, 1968). These models have provided the basis for a theory of dendritic function (Rall et al., 1995).

SPREAD OF STEADY-STATE SIGNALS

Cable Theory Depends on Simplifying Assumptions

The successful application of cable theory to neurons requires that it be based as closely as possible on the structural and functional properties of dendritic processes, despite their obvious complexity. The key to describing the spread of electrical current through dendrites is a set of carefully chosen simplifying assumptions, which allow the construction of an *equivalent circuit* of the electrical properties of such a segment. These are summarized in Box 17.1 (Rall et al., 1995).

From Molecules to Networks.
DOI: http://dx.doi.org/10.1016/B978-0-12-397179-1.00017-8

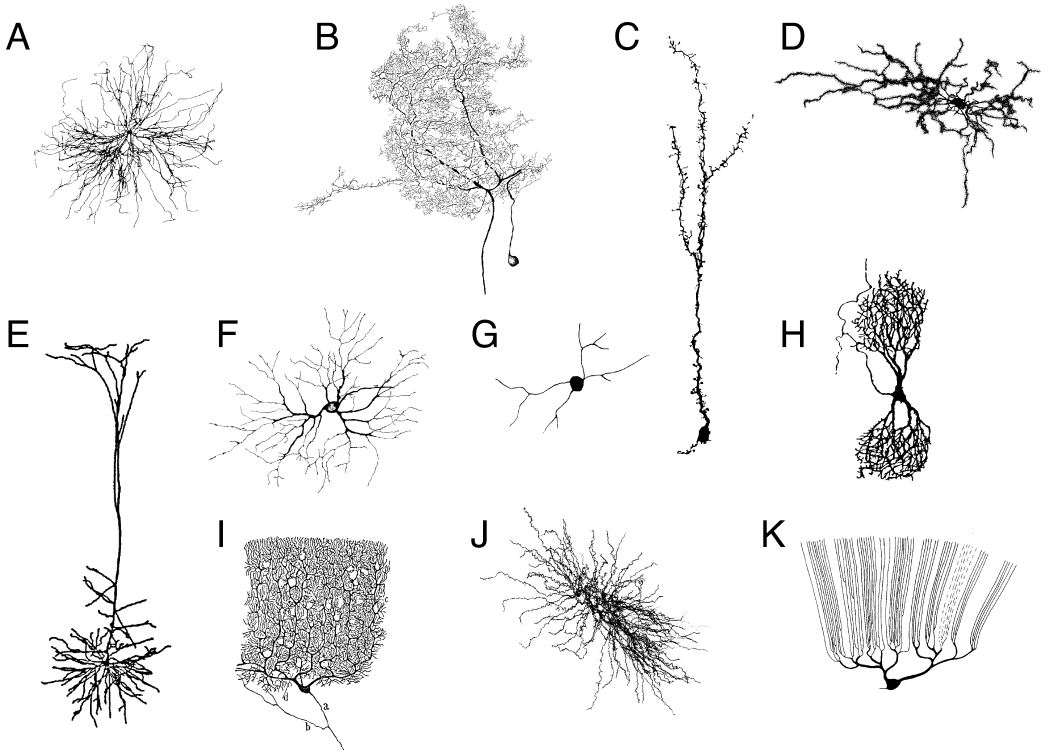

FIGURE 17.1 **Cell-type specific dendritic arborizations.** (A) Alpha motor neuron in cat spinal cord. (B) Interneuron in locust mesothoracic ganglion. (C) Granule cell in mouse olfactory bulb. (D) Spiny projection neuron in rat striatum. (E) Layer 5 pyramidal cell in rat neocortex. (F) Ganglion cell in cat retina. (G) Amacrine cell in salamander retina. (H) Neuron in human nucleus of Burdach. (I) Purkinje neuron in human cerebellum. (J) Relay neuron in rat ventrobasal thalamus. (K) Purkinje neuron in mormyrid fish. *Adapted from Mel (1994).*

Electrotonic Spread Depends on the Characteristic Length Constant

We begin by using the assumptions in Box 17.1 to represent a segment of a process by electrical resistances: an internal resistance r_i connected to the r_i of the neighboring segments and through the membrane resistance r_m to ground (see Fig. 17.3B). We will first consider the spread of electrotonic potential under steady-state conditions (Fig. 17.3C). In standard cable theory, this is described by

$$V = \frac{r_m}{r_i} \cdot \frac{d^2V}{dx^2} \tag{17.1}$$

This equation states that if there is a steady-state current input at point $x = 0$, the electrotonic potential (V) spreading along the cable is proportional to the second derivative of the potential (d^2V) with respect to distance and the ratio of the membrane resistance (r_m) to the internal resistance (r_i) over that distance. The steady-state solution of this equation for a cable of infinite extension for positive values of x gives

$$V = V_0\, e^{-x/\lambda}, \tag{17.2}$$

where λ is defined as the square root of r_m/r_i (in centimeters) and V_0 is the value of V at $x = 0$.

Inspection of this equation shows that when $x = \lambda$, the ratio of V to V_0 is $e^{-1} = 1/e = 0.37$. Thus, λ is a critical parameter defining the length over which the electrotonic potential spreading along an infinite cable decays (is attenuated) to a value of 0.37 of the value at the site of the input. It is referred to as the *characteristic length constant* of the cable. The higher the value of the specific membrane resistance (R_m), the higher the value of r_m for that segment, the larger the value for λ, and the greater the spread of electrotonic potential through that segment (Fig. 17.4). Specific membrane resistance (R_m) is thus an important variable in determining how efficient activity can spread through a dendritic tree.

Most of the electrotonic current crossing the membrane may be carried by K^+ "leak" channels, which are largely responsible for holding the cell at its resting potential. However, the dendrites of a cell are targeted by numerous synapses, whose activation will lead to the opening of a variety of additional ligand and voltage-gated channels. Thus, the effective R_m can vary from values of less than 1,000 Ωcm^2 to more than 100,000 Ωcm^2 at different times and in different subregions of a dendritic tree. Note that λ varies with the square root of R_m, so a 100-fold difference in R_m translates into only a 10-fold difference in λ.

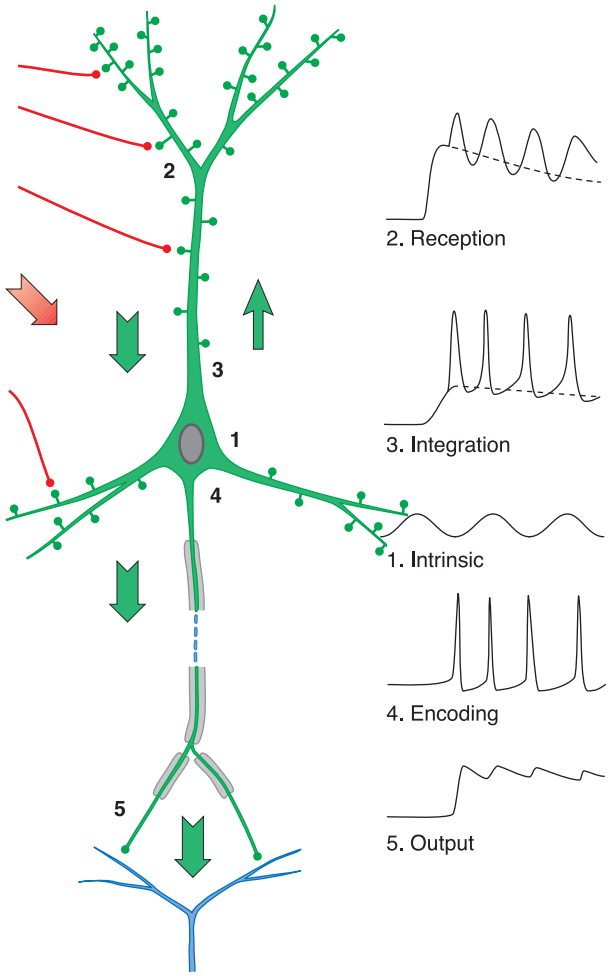

FIGURE 17.2 **Neurons have four main regions and five main functions.** Electrotonic potential spread is fundamental for coordinating the regions and their functions. See text for details.

Conversely, the higher the value of the specific internal resistance (R_i), the higher the value of r_i for that segment, the smaller the value of λ, and the less the spread of electrotonic potential through that segment. The value of R_i in mammalian neurons is estimated to be at 200 Ωcm. Unlike R_m, biological changes in R_i are assumed to be small and are therefore not critical in determining changes in the spread of current through dendritic trees. However, the presence of intracellular organelles in the cytoplasm may alter the effective R_i, particularly for very thin processes, such as distal dendritic branches.

Electrotonic Spread Depends on the Diameter of a Process

The length constant (λ) depends not only on the internal and membrane resistance, but also on the diameter of a process. Thus, from the relations between r_m and R_m, and r_i and R_i, discussed in the preceding section,

$$\lambda = \sqrt{\frac{r_m}{r_i}} = \sqrt{\frac{R_m}{R_i} \cdot \frac{d}{4}} \qquad (17.3)$$

Neuronal processes vary widely in diameter. In the mammalian nervous system, the thinnest processes are the distal branches of dendrites and the necks of some dendritic spines; these processes may have diameters of only 0.1 μm or less. In contrast, the largest dendritic trunks of mammalian neurons may have diameters as large as 20 to 25 μm. This means that the range of diameters is approximately three orders of magnitude (1,000-fold). Note, again, that λ varies with the square root of d; thus, for a 10-fold change in diameter, the change in λ is only about 3-fold.

SPREAD OF TRANSIENT SIGNALS

Electrotonic Spread of Transient Signals Depends on Membrane Capacitance

Until now, we have considered only the spread of steady-state inputs. However, most neural signals change rapidly. In mammalian neurons, fast synaptic potentials last from 1 to 30 milliseconds. The spread of such transient signals through the dendritic tree not only depends on all of the factors discussed for steady-state signals, but also on the membrane capacitance (c_m), which is due to the lipid moiety of the plasma membrane. The value for the specific membrane capacitance (C_m) is estimated at $\sim 1\ \mu F/cm^2$.

The simplest case demonstrating the effect of membrane capacitance on transient signals is that of a single segment. In the equivalent electrical circuit for a neural process, the membrane capacitance is placed in parallel with ohmic components of the membrane conductance and the driving potentials for ion flows through those conductances (Fig. 17.3B). Again neglecting the resting membrane potential, we take as an example the injection of a current step into a segment; in this case, the time course of the current spread to ground is described by the sum of the capacitive and resistive current (plus the input current, I_{pulse}):

$$C\frac{dV_m}{dt} + \frac{V_m}{R} = I_{pulse} \qquad (17.4)$$

Rearranging,

$$RC\frac{dV_m}{dt} + V_m = I_{pulse} \cdot R, \qquad (17.5)$$

where $RC = \tau$ (τ is the time constant of the membrane).

BOX 17.1

BASIC ASSUMPTIONS UNDERLYING CABLE THEORY

1. **Segments are cylinders**. A segment is assumed to be a cylinder with constant radius.

   This is the simplest assumption; however, compartmental simulations can readily incorporate different geometrical shapes with differing radii if needed (Fig. 17.3B).

2. **The electrotonic potential is due to a change in the membrane potential.** At any instant of time, the "resting" membrane potential (E_r) at any point on the neuron can be changed by several means: injection of current into the cell, extracellular currents that cross the membrane, and changes in membrane conductance (caused by a driving force different from that responsible for the membrane potential). Electric current then begins to spread between that point and the rest of the neuron, in accord with

   $$V = V_m - E_r$$

   where V is the electrotonic potential and V_m is the changed membrane potential.

   Since membrane potential is rarely at rest under physiological conditions, "resting" potential refers to the membrane potential at any given instant of time other than during an action potential or rapid synaptic potential.

3. **Electrotonic current is ohmic**. Passive electrotonic current flow is usually assumed to be ohmic, i.e., in accord with the simple linear equation

   $$E = IR,$$

   where E is the potential, I is the current, and R is the resistance. This relation is largely inferred from macroscopic measurements of the conductance of solutions having the composition of the intracellular medium, but is rarely measured directly for a given nerve process. Also largely untested is the likelihood that at the smallest dimensions (0.1 μm diameter or less), the processes and their internal organelles may acquire submicroscopic electrochemical properties that deviate significantly from macroscopic fluid conductance values; compartmental models permit the incorporation of estimates of these properties.

4. **In the steady state, membrane capacitance is ignored**. The simplest case of electrotonic spread occurs from the point on the membrane of a steady-state change (e.g., due to injected current, a change in synaptic conductance, or a change in voltage-gated conductance) so that time-varying properties (transient charging or discharging of the membrane) due to the membrane capacitance can be ignored (Fig. 17.3C).

5. **The resting membrane potential can usually be ignored**. In the simplest case, we consider the spread of electrotonic potential (V) relative to a uniform resting potential (E_r) so that the value of the resting potential can be ignored. Where the resting membrane potential may vary spatially, V must be defined for each segment as

   $$V = E_m - V_r$$

6. **Electrotonic current divides between internal and membrane resistance**. In the steady state, at any point on a process, current divides into two local resistance paths: further within the process through an internal (axial) resistance (r_i) or across the membrane through a membrane resistance (r_m) (see Fig. 17.3C).

7. **Axial resistance is inversely proportional to diameter.** Within the volume of the process, current is assumed to be distributed equally (in other words, the resistance across the process, in the Y and Z axes, is essentially zero). Because resistances in parallel sum reciprocally to decrease the overall resistance, axial current (I) is inversely proportional to the cross-sectional area ($I \propto \frac{1}{A} \propto \frac{1}{\pi r^2}$); thus, a thicker process has a lower overall axial resistance than a thinner process. Because the axial resistance (r_i) is assumed to be uniform throughout the process, the total cross-sectional axial resistance of a segment is represented by a single resistance,

   $$r_i = R_i/A,$$

   where r_i is the internal resistance per unit length of cylinder (in ohms per centimeter of axial length), R_i is the specific internal resistance (in Ωcm), and A ($=\pi r^2$) is the cross-sectional area.

   The internal structure of a process may contain membranous or filamentous organelles that can raise the effective internal resistance. In voltage-clamp experiments, the space clamp eliminates current through r_i, so that the only current remaining is through r_m, thereby permitting isolation and analysis of different ionic membrane conductances, as in the original experiments of Hodgkin and Huxley (Fig. 17.3D).

8. **Membrane resistance is inversely proportional to membrane surface area.** For a unit length of

BOX 17.1 (*cont'd*)

cylinder, the membrane current (i_m) and the membrane resistance (r_m) are assumed to be uniform over the entire surface. Thus, by the same rule of the reciprocal summing of parallel resistances, the membrane resistance is inversely proportional to the membrane area of the segment so that a thicker process has a lower overall membrane resistance. Thus,

$$r_m = R_m/c,$$

where r_m is the membrane resistance for unit length of cylinder (in Ωcm of axial length), R_m is the specific membrane resistance (in Ωcm^2), and c ($=2\pi r$) is the circumference. For a segment, the entire membrane resistance is regarded as concentrated at one point; i.e., there is no axial current flow within a segment but only between segments (see Fig. 17.3C).

Membrane current passes through ion channels in the membrane. The density and types of these channels vary in different processes and indeed may vary locally in different segments and branches. These differences are incorporated readily into compartmental representations of the processes.

9. **The external medium along the process is assumed to have zero resistivity.** In contrast with the internal axial resistivity (r_i), which is relatively high because of the small dimensions of most nerve processes, the external medium has a relatively low resistivity for current because of its relatively large volume. For this reason, the resistivity of the paths either along a process or to ground is generally regarded as negligible, and the potential outside the membrane is assumed to be equivalent to ground (see Fig. 17.3C). This greatly simplifies the equations that describe the spread of electrotonic potentials inside and along the membrane.

   Compartmental models can simulate any arbitrary distribution of properties, including significant values for extracellular resistance where relevant. Particular cases in which external resistivity may be large, such as the special membrane caps around synapses on the cell body or axon hillock of a neuron, can be addressed by suitable representation in the simulations. However, for most simulations, the assumption of negligible external resistance is a useful simplifying first approximation.

10. **Driving forces on membrane conductances are assumed to be constant**. It is usually assumed that ion concentrations across the membrane are constant during activity.

    Changes in ion concentrations with activity may occur, particularly in constricted extracellular or intracellular compartments; these changes may cause deviations from the assumptions of constant driving forces for the membrane currents, as well as the assumption of uniform E_r. For example, accumulations of extracellular K^+ during periods of sustained neuronal activity may change local E_r, and intracellular accumulations of ions within the tiny volumes of spine heads may change the driving force on synaptic currents. These special properties are easily included in most compartmental models.

11. **Cables have different boundary conditions**. In classical electrotonic theory, cables are assumed to have infinite length (one customarily assumes a semi-infinite cable with $V = 0$ at $x = 0$ and only positive values of length x). This assumption carries over to the application of cable theory to long axons, but most dendrites are relatively short. This imposes boundary conditions on the solutions of the cable equations, which have very important effects on electrotonic spread.

    In highly branched dendritic trees, boundary conditions are difficult to deal with analytically but are readily represented in compartmental models.

The solution of this equation for the response to a step change in current (I) is

$$V_m(T) = I_{pulse}\, R\left(1 - e^{-T}\right), \tag{17.6}$$

where $T = t/\tau$.

When the pulse is terminated, the decay of the initial potential (V_0) to rest is given by

$$V_m(T) = V_\infty e^{-T} \tag{17.7}$$

These "on" and "off" transients are shown in Fig. 17.5. The significance of τ is shown in the diagram; it is the time required for the voltage change across the membrane to reach $1/e = 0.37$ of its final value. The membrane time constant defines the step-evoked voltage response of a membrane segment in terms of its electrotonic properties. It is analogous to the way that the length constant defines the spread of voltage change over distance.

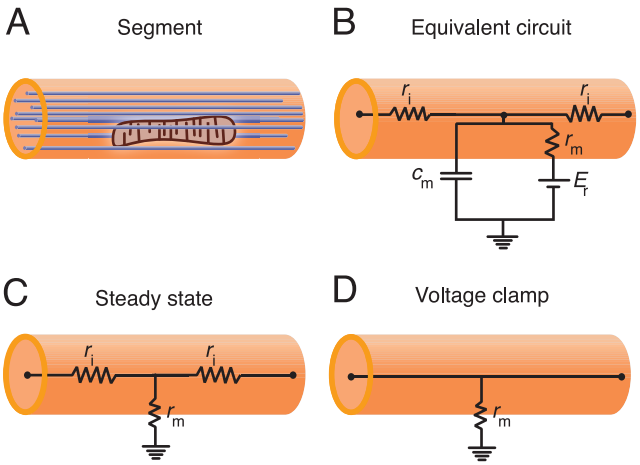

FIGURE 17.3 Steps in construction of a compartmental model of the passive electrical properties of a dendritic branch. (A) Schematic of a dendritic segment and its organelles. (B) Abstraction of an equivalent electrical circuit based on the membrane capacitance (c_m), membrane resistance (r_m), resting membrane potential (E_r), and internal resistance (r_i). (C) Abstraction of the circuit for steady-state electrotonus, in which c_m and E_r can be ignored. (D) The space clamp used in voltage-clamp analysis reduces the equivalent circuit even further to only the membrane resistance (r_m), usually depicted as membrane conductances (g) for different ions.

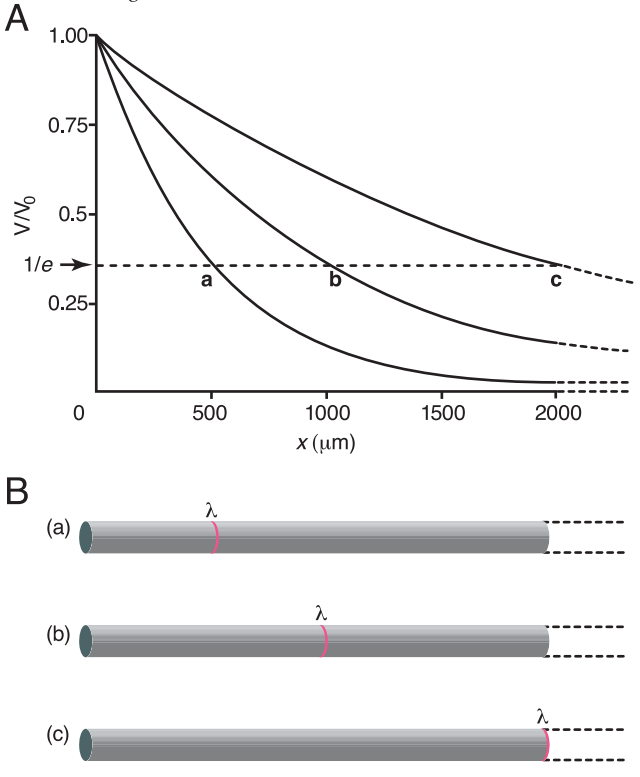

FIGURE 17.4 The decay of membrane potential along an infinite dendritic cable is described by the length constant. (A) Membrane potential as function of distance along the dendrite, with the site of current injection at $x = 0\,\mu m$. Potential profiles for processes with three different values of λ are shown (a–c). At the distance of λ, the membrane depolarization is $1/e$ of that at the origin. (B) Lines indicate the location of λ (one length constant) for three dendritic processes with potentials profiles shown in (A).

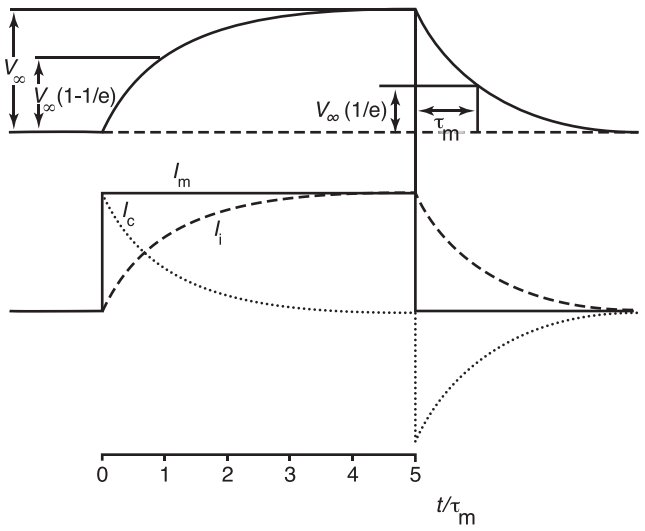

FIGURE 17.5 The equivalent circuit of a single isolated compartment responds to an injected current step by charging and discharging with a time course determined by the time constant, τ. Top trace shows the voltage response of the compartment. Bottom traces show the time course for the resistive and the capacitive current which underlie the voltage response. V_∞ = steady-state voltage in response to the current pulse; I_m = injected current applied to membrane; I_c = current through the capacitance; I_i = current through the ionic leak conductance; τ_m = membrane time constant. *From Jack et al. (1975).*

A Two-Compartment Model Defines the Basic Properties of Dendritic Signal Spread

These spatial and temporal cable properties can be combined in a two-compartment model that can be applied to the generation and spread of any arbitrary transient signal (Fig. 17.6).

In the simplest case, current is injected into one of the compartments, as in an electrophysiological experiment. Positive charge injected into compartment A attempts to flow outward across the membrane, partially opposing the negative charge on the inside of the lipid membrane (the charge responsible for the negative resting potential), thereby depolarizing the membrane capacitance (C_m) at that site. At the same time, the charge begins to flow as current across the membrane through the resistance of the ionic membrane channels (R_m) that are open at that site. The proportion of charge divided between C_m and R_m determines the rate of charge of the membrane, i.e., the membrane time constant, τ. However, charge also starts to flow through the internal resistance (R_i) into compartment B, where the current again divides between capacitance and resistance. The charging (and discharging) transient in compartment A differs from the time constant of a single isolated compartment, being faster because the rest of the cable (represented by compartment B) represents a "current sink."

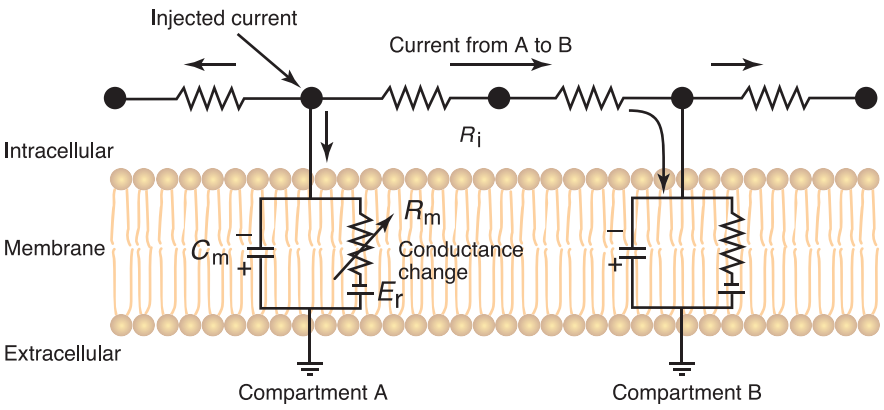

FIGURE 17.6 **The equivalent circuit of two neighboring compartments or segments** (A and B) of a dendrite shows the pathways for current spread in response to an input (injected current or increase in membrane conductance) at segment A. See text for details.

This case is a useful starting point because an experimenter often injects electrical currents into a cell to analyze neuronal properties. However, a neuron normally generates current spread by means of localized conductance changes across the membrane. In Fig. 17.6, consider an excitatory postsynaptic potential, producing an inward positive current in compartment A. The charge transferred to the interior surface of the membrane will follow the same paths as outlined for the injected current by opposing the negativity inside the membrane capacitance, crossing the membrane through the open membrane channels, and spreading through the internal resistance to the next compartment, where the charge flows are similar.

Thus, the two cases start with different means of transferring positive charge into the cell, but from that point the current paths and the associated spread of the electrotonic potential are similar. The electrotonic current that spreads between the two segments is referred to as the *local current*. The charging transient in compartment A is faster than the time constant of the resting membrane; this difference is due both to the current sink generated by compartment B (as in the injected current case) and to the fact that the imposed conductance increase in compartment A reduces the membrane time constant (by reducing effective R_m). This illustrates a critical point first emphasized by Wilfrid Rall (1964): changes in membrane conductance alter the electrotonic structure so that it no longer acts as a linear system, even though it remains entirely passive. This behavior is critical to understand nonlinear summation of synaptic responses, as discussed below.

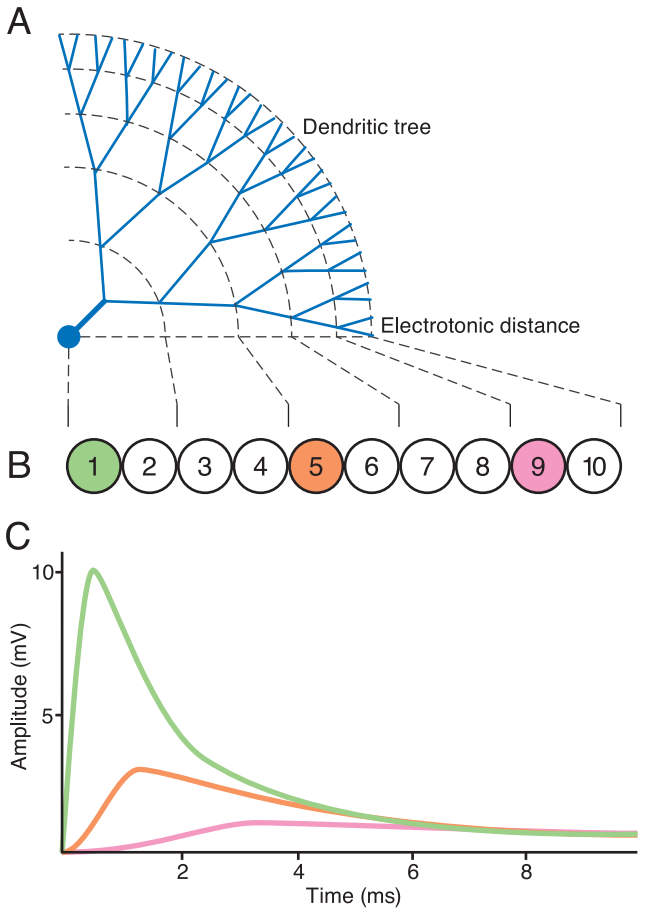

FIGURE 17.7 **The spread of electrotonic potentials is accompanied by a delay and an attenuation of amplitude.** (A) Schematic of a dendritic tree. An excitatory postsynaptic potential (EPSP) is generated in compartment 1, 5, or 9 (B) while recordings are made from compartment 1. (C) Short latency, large amplitude, and rapid transient response in compartment 1 at the site of input, as well as the later, smaller, and slower responses recorded in compartment 1 for the same input to compartments 5 and 9. *Based on Rall (1967).*

Dendritic Synaptic Potentials are Delayed and Attenuated by Electrotonic Spread

We can now assess the effects of cable properties on the spread of synaptic potentials through dendritic branches and trees. Consider the case of recording from the cell body of a model neuron while delivering a brief excitatory synaptic conductance to different locations in the dendritic tree (Fig. 17.7). The somatic response to a conductance at the nearest site is a synaptic potential with rapid rise and decay. When the

input is delivered to the middle of the chain of compartments, the response in the soma begins only after a delay, rises more slowly, reaches a much lower peak, and decays slowly toward baseline. For input to the terminal compartment, the voltage delay at the soma is so long that the response has barely started by the end of the synaptic conductance change in the distal dendrite; the response rises slowly to a delayed and prolonged plateau that subsides very slowly.

For synapses placed at increasing distance from the soma there are also important changes in the *local* voltage response. In distal dendritic branches, the high input impedance combined with a low overall capacitance produces a very large voltage change for any given synaptic conductance change. This has important consequences for the synaptic activation of voltage-dependent conductances expressed in dendrite and spines, as we will see in later sections. Balanced against this high input resistance is a second factor: the small branch has a very large conductance load on it because of the presence of the dendritic tree. As a result, there is a steep decrement in the electrotonic potential spreading from the branch through the tree toward the cell body.

For a transient synaptic input, a third factor— membrane capacitance—must be taken into account. In spreading from a small process (such as a distal dendrite or spine), the transient synaptic potential is attenuated by the impedance mismatch between the process and the rest of the dendritic tree. Spread of the transient signal through the dendritic tree is attenuated further by the need to charge the capacitance of the dendritic membrane and is slowed by the time taken for the charging (Fig. 17.7C).

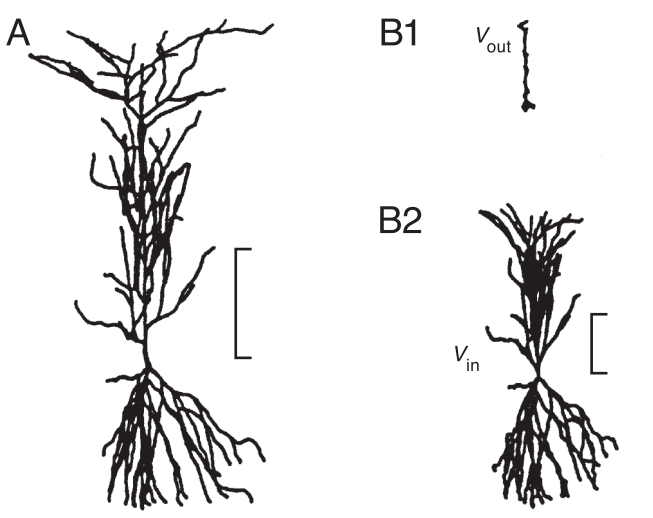

FIGURE 17.8 **The electrotonic structure of a neuron varies with the direction of spread of signals.** (A) Stained CA1 pyramidal neuron. Calibration bar, 200 μm (B) Electrotonic transform of the stained morphology for the case of a voltage spreading away from the cell body (B1, V_{out}) and toward the cell body (B2, V_{in}). Calibration bar, 1 electrotonic length. *From Carnevale et al. (1997).*

DYNAMIC PROPERTIES OF THE PASSIVE ELECTROTONIC STRUCTURE

Electrotonic Structure of the Neuron Changes Dynamically

It should now be obvious that the electrotonic structure of a dendritic tree is not fixed, but varies based on the kinetics of the signals that spread through the dendritic tree, the direction of signal flow, and the dynamic changes in effective membrane resistance. This can be illustrated graphically for the entire soma-dendritic system by starting with the neuronal morphology and modifying its size according to its electrotonic properties (Zador et al., 1995). This is termed a *morphoelectrotonic transform* (MET).

As an example, MET can be used to visualize how the electrotonic structure of a neuron depends on the direction of signal spread. Fig. 17.8 shows a CA1 hippocampal pyramidal cell for which a comparison is made between spread of a steady-state signal from the soma to the dendrites (voltage out, V_{out}) with spread from the dendrites to the soma (voltage in, V_{in}). On the left (Fig. 17.8A) is the stained neuron, with its long and highly branched apical dendrite and its more compact basal dendritic tree. Fig. 17.8B2 illustrates an electrotonic representation of the neuron for signals spreading from the distal dendrites toward the soma. There is severe decrement from each distal branch so that apical and basal dendritic trees have electrotonic lengths of approximately 3 and 2, respectively. By comparison, Fig. 17.8B1 illustrates the electrotonic representation of this neuron for a steady-state signal spreading from the soma into the dendrites. The basal dendrites have been reduced to almost nothing, indicating that they are nearly isopotential with the cell body. This property emerges because the branches are relatively short compared with their electrotonic lengths and because the terminal branches lead to more current crossing the membrane, thereby greatly reducing the decrement of electrotonic potential. The apical dendrite has shrunk to an electrotonic length of approximately 1. Qualitatively similar observations can be made for transient signals such as postsynaptic responses or action potentials. Thus, the two METs illustrate the strong attenuation experienced by voltage signals from the dendrites towards the soma, whereas signal flow from the soma into the dendrites is considerably more efficient.

Synaptic Conductances in Dendritic Trees Tend to Interact Nonlinearly

It is often assumed that synaptic responses sum linearly, but that this is not generally true. Synaptic responses generate current by means of the opening of ionotropic or metabotropic conductances, which alters the overall membrane resistance of that segment, thereby changing the electrotonic properties of the whole system. This effect is illustrated by the two-compartment model in Fig. 17.6. Consider a synaptic input to compartment A, which decreases the membrane resistance of that compartment. Now assume a simultaneous synaptic input to compartment B, which has the same effect on the membrane resistance of that compartment. The internal current flowing between the two compartments encounters much lower impedance and hence has much less effect on the membrane potential than would have been the case for current injection. The integration of these two responses therefore gives a smaller, sublinear potential compared to the linear summation of the two individual responses. In essence, each compartment partially short circuits the other through a larger conductance load, thus reducing the combined response.

As a result, synaptic integration in dendrites is usually not linear, even assuming purely passive membrane properties. The further apart the synaptic sites, the smaller the interactions between the conductances, and the more linear the summation becomes (see Fig. 17.9A, B). Such distance-dependent nonlinear summation has been observed in neurons of the auditory brainstem, which are involved in computing the location of sound in space. These neurons act as coincidence detectors and respond maximally when they receive simultaneous inputs from both ears (Agmon-Snir et al., 1998). The sensitivity to binaural inputs is in part mediated by the cell morphology and a unique arrangement of synaptic inputs (Fig. 17.9C). Binaural neurons form two main dendrites, with each dendrite receiving synaptic afferents only from one ear. Simultaneous inputs from both ears arrive at the two dendrites at a large intersynaptic distance and are summed up at the soma in a near-linear manner, triggering the generation of action potentials. However, for simultaneous inputs arriving from the same ear, summation is sublinear, due to a smaller intersynaptic distance. As a result, inputs from the same ear generate smaller somatic response that fails to trigger action potentials (Fig. 17.9C).

Even in neurons without such a clear separation of synaptic afferents onto different dendrites, the relative placement of synaptic inputs determines the degree of their interaction. Neocortical and hippocampal pyramidal cells form extensive basal dendritic trees (Fig. 17.1C) that receive the majority of excitatory and inhibitory synaptic inputs. As illustrated in Fig. 17.10, synaptic inhibition has little effect on synaptic excitation when the two types of synapses are targeted to

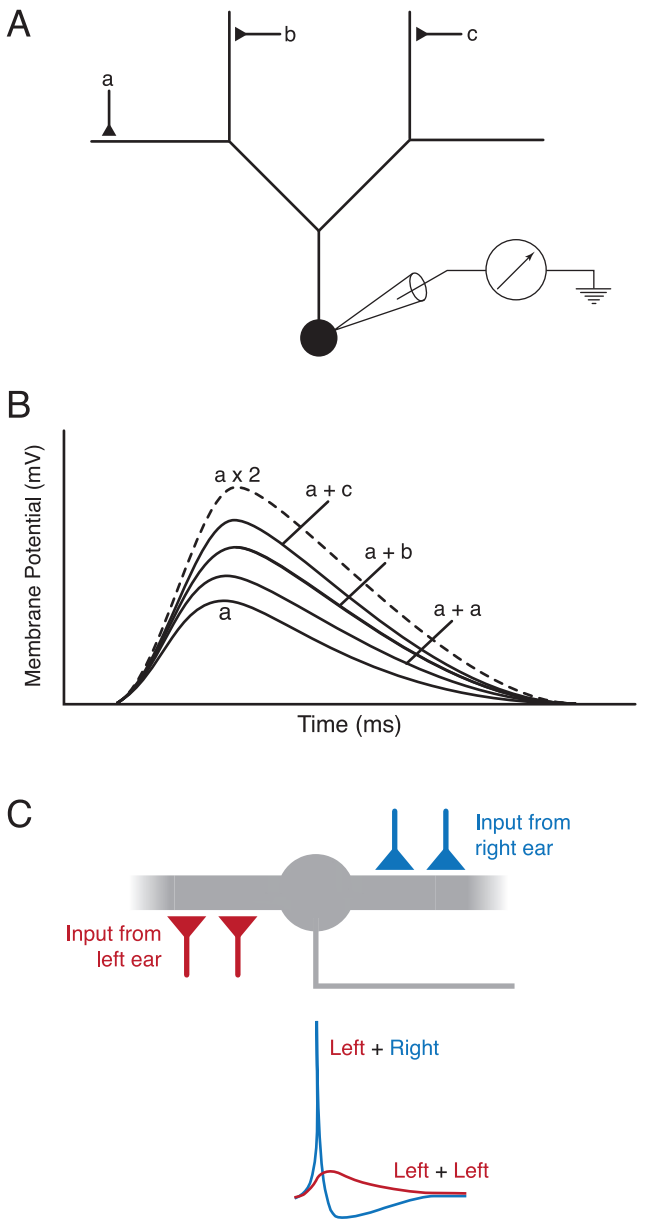

FIGURE 17.9 Schematic diagram of a dendritic tree to illustrate graded effects of nonlinear interactions between synaptic conductances. (A) Three sites of synaptic input (a–c) are shown, with a recording site in the soma. (B) Somatic responses evoked by different combinations of inputs: (a) single input at a; (a + a) double the conductance at a; (a + b, a + c) simultaneous inputs at synaptic sites with increasing distance; (a × 2) linear doubling of a. The largest somatic response is generated by synaptic inputs with the largest spatial separation, which minimizes the interaction of conductances. *From Shepherd and Koch (1990).* (C) For binaural neurons in the auditory brainstem, simultaneous inputs from one ear target the same dendrite and summate sublinearly, whereas simultaneous inputs to both ears contact separate dendrites and summate in a near-linear manner, triggering postsynaptic action potentials. *Adapted from London and Hausser (2005).*

different dendritic branches, but a profound effect when both inputs are located on the same branch. In the mammalian brain, fast inhibition is primarily mediated by the activation of $GABA_A$ receptors, whose activation will generate a conductance change with a reversal potential close to the resting potential of the membrane. Such "shunting" inhibition has important functional consequences, being effective only during the brief period the GABAergic conductance is open and controlling excitation only in specific dendritic subregions.

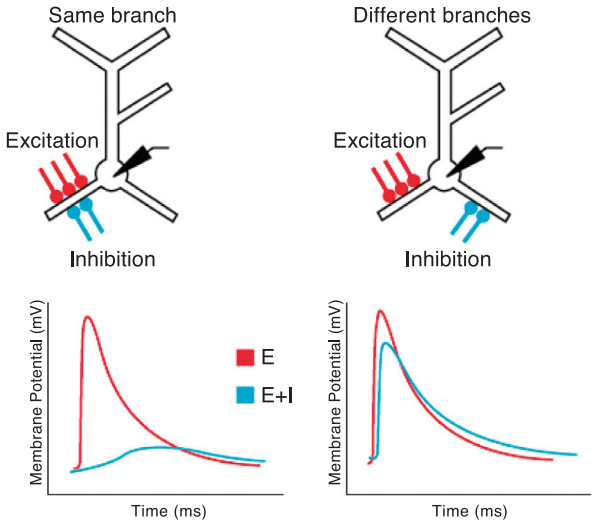

FIGURE 17.10 **Importance of the locations of interacting synaptic responses within a dendritic tree.** Left, Excitation and inhibition converging on the same dendritic branches produces sharp reduction of the excitatory response recorded at the soma. Right, inhibition on a different set of branches has little effect in reducing the excitatory response recorded at the soma. *From Mel and Schiller (2004).*

Dendritic Spines Form Electrotonic and Biochemical Compartments

The rules governing electrotonic interactions within a dendritic tree also apply at the level of a spine, the smallest process of a neuron. Dendritic spines are the target for most excitatory inputs in pyramidal neurons in the cerebral cortex and in cerebellar Purkinje cells, as well as in a variety of other neuron types, so an understanding of their properties is critical for understanding brain function (Alvarez and Sabatini, 2007; Araya et al., 2006; Shepherd, 1996). Generally spines consist of a distinct head (<1 μm diameter), connected to the parent dendritic branch via a narrow neck (<0.2 μm diameter). As with the whole dendritic tree, understanding the functional properties of spines is facilitated by first characterizing their electrotonic properties. Given the set of principles we have generated earlier in this chapter, by simple inspection of spine morphology as shown in Fig. 17.11, we can postulate several distinctive features that may have important functional implications (see Box 17.2).

In addition to its electrotonic properties, the spine has interesting biochemical properties. The same cable equations that govern electrotonic properties also have their counterparts in describing the diffusion of substances. Thus, accumulations of only small numbers of ions are needed within the tiny volumes of spine heads to change the driving force on an ion species or to affect significant changes in the concentrations of subsequent second messengers. As outlined later in this chapter, interest in the biochemical signaling within spines is intensifying, as our ability to image ion fluxes, such as for Ca^{2+}, and to measure other molecular properties of individual spines increases

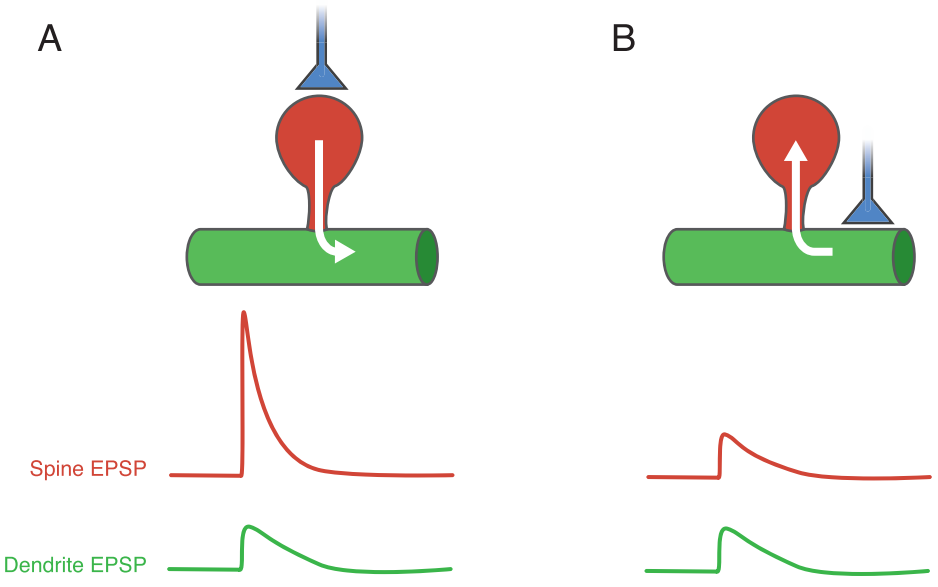

FIGURE 17.11 **Spines dramatically increase local postsynaptic responses.** (A) Excitatory synapse targeted to spine produces a large and fast local depolarization, due to the high input impedance and the small membrane capacitance of the spine head. (B) The same synapse placed onto a dendritic branch generates a small local EPSP with virtually no voltage drop as current flows into the spine. Note that while the local EPSP amplitude at the site of the synaptic input is strongly influenced by the geometry of the postsynaptic compartment, the responses in the parent dendrite (green traces) and the soma are similar regardless of synapse placement, due to negligible charge loss. *Adapted from Spruston (2008).*

BOX 17.2

BASIC ELECTROTONIC PROPERTIES OF DENDRITIC SPINES

1. **High input resistance.** The smaller the size and the narrower the stem, the higher the input resistance; this property leads to a large amplitude local synaptic potential for a given synaptic conductance (Fig. 17.11) Such a large depolarizing EPSP can have powerful effects on activating voltage-dependent conductances within the spine.
2. **Low total membrane capacitance.** The small size also means a small total membrane capacitance, implying that synaptic (and any active) potentials may be rapid; this means that spines on dendrites can potentially be involved in rapid information transmission.
3. **Increases in total dendritic membrane capacitance.** Although the membrane capacitance of an individual spine is small, the combined spine population increases the total capacitance of its parent dendrite. This property increases the filtering effect of the dendrite on transmission of signals through it.
4. **Decrement of potentials spreading from the spine.** An impedance mismatch exists between the spine head and its parent dendrite; this means that potentials spreading from the spine to the dendrite will suffer considerable decrement unless there are active properties of the dendrite or of neighboring spines to boost the signal.
5. **Ease of potential spread into the spine**. The other side of the impedance mismatch is that membrane potential changes within the dendrite spread into the spine with little decrement; thus, the spine tends to follow the potential of its dendrite (Fig. 17.11B). This property means that a spine can serve as a coincidence detector for nearby synaptic responses or for an action potential backpropagating into the dendritic tree.
6. **Linearization of synaptic integration.** The location of excitatory synapses on spines increases their anatomical and electrotonic distance, thereby decreasing the interactions between their conductances, producing a more linear interaction of the postsynaptic responses.

with new technology such as multiphoton microscopy. The interpretation of those results for the integrative properties of the neuron will require considerations in the biochemical domain that parallel those discussed in the electrotonic domain.

ACTIVE DENDRITIC PROPERTIES

While intracellular recordings from the cell bodies of many neurons have long provided clues that dendritic integration is not a passive process, only direct dendritic recordings and imaging techniques have provided conclusive evidence that dendrites can express a number of different types of voltage- and Ca^{2+}-gated conductances, with important consequences for the processing of signals in dendritic trees and neuronal output.

There are two main challenges with studying the active properties of dendrites. One is technical. Dendrites are small, so examining their electrical properties with recording electrodes has long been limited to dendritic processes with unusually large diameter. In recent years, electrophysiological techniques have dramatically improved and dendritic recordings from an increasing number of neuronal types can now be obtained routinely (Davie et al., 2006). In addition, a number of high-resolution imaging techniques such as multiphoton microscopy allow for measurements of Ca^{2+} influx in spines and thin dendrites, which are not accessible to direct recordings (Denk and Svoboda, 1997). However, these advances have only highlighted a second major challenge. Neurons express a plethora of different types of voltage and Ca^{2+} gated ion channels in their dendrites, often in nonuniform distributions, with dramatic differences between different cell types. Moreover, these channel distributions are highly plastic and can be modified during development or as a result of different types of cellular learning. Similar to dendritic morphology, active dendritic properties are thus highly diverse and dynamic, likely a reflection of their critical role in dendritic processing. This complexity has made it difficult to define a set of general rules underlying dendritic function.

Nevertheless, for a number of model systems the detailed distributions of different conductances, as well as their possible functional roles are now reasonably well understood. These include pyramidal cells in neocortex and hippocampus, Purkinje neurons of the cerebellar cortex, and mitral/tufted cells of the olfactory bulb. In the next section, we will briefly review the types of voltage- and Ca^{2+}-gated ion channels commonly observed in dendrites of several types of

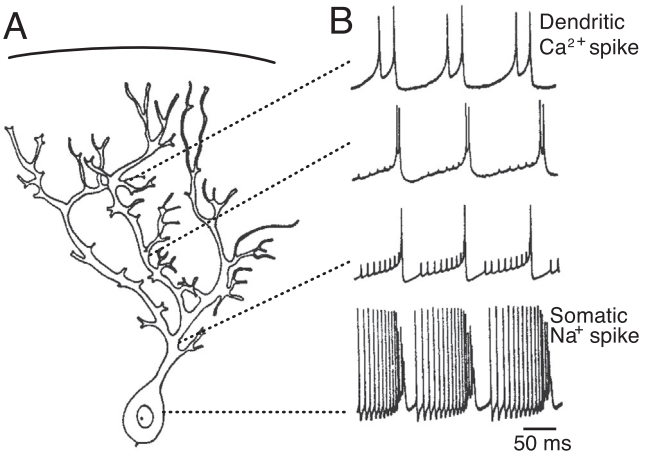

FIGURE 17.12 **Demonstration of active dendrites via direct dendritic recordings.** (A) Drawing of a Purkinje cell in the cerebellar cortex. (B) Intracellular recording from the soma (bottom trace) showing fast Na^+ spikes. Recordings from dendritic sites at increasing distance from the soma indicate progressively smaller fast events and increasingly larger slow Ca^{2+} spikes. *From Llinás and Sugimori (1980).*

mammalian neurons and describe how their presence can shape neuronal processing. Excellent reviews on the functional role of active dendrites have been published in recent years (London and Hausser, 2005; Magee, 2000; Spruston, 2008; Stuart et al., 2007).

Dendritic Na^+ Channels

TTX sensitive Na^+ channels are expressed in fairly uniform density in the dendritic trees of many neurons, including pyramidal cells, mitral cells of the olfactory bulb, dopaminergic neurons of the substantia nigra, and GABAergic interneurons in the hippocampus and the thalamus. Notable exceptions are the dendrites of Purkinje neurons, which contain only a very low Na^+ channel density (Fig. 17.12). As discussed below, high-threshold and fast inactivating dendritic Na^+ currents allow for the propagation of action potentials from their initiation site (typically the axon) into the dendritic tree. In addition, neurons such as pyramidal cells also can generate a persistent Na^+ current that activates below spike threshold and inactivates only slowly, suggesting a role in boosting subthreshold postsynaptic responses. Na^+ channel dependent dendritic boosting occurs particularly during sustained synaptic activity (Oviedo and Reyes, 2002), which favors activation of the persistent Na^+ current, whereas Na^+ current-dependent dendritic boosting for a single EPSP is minimal (Stuart and Sakmann, 1995).

Dendritic Ca^{2+} Channels

Electrical responses mediated by the opening of voltage-gated Ca^{2+} channels expressed in dendrites can influence dendritic excitability much in the same way as Na^+ channels. However, by generating significant increases in dendritic Ca^{2+} concentration, Ca^{2+} channel opening can also control an enormous range of biochemical cascades. Ca^{2+} channels can vary dramatically in the voltage required for their activation and the degree to which they inactivate following depolarization (see also Chapter 13). For example, T-type Ca^{2+} channels are low-threshold conductances that can be activated by modest depolarization from resting membrane potentials but experience rapid inactivation. These conductances are expressed in the dendrites of hippocampal neurons, mitral and granule cells of the olfactory bulb and the dendrites of thalamic neurons. Their low activation threshold allows for their recruitment by small amplitude postsynaptic responses, suggesting that they play a role in the amplification of excitatory synaptic inputs (Gillessen and Alzheimer, 1997). In some neurons, activation of dendritic T-type channels is responsible for the generation of Ca^{2+} spikes underlying burst firing in the soma.

Dendrites can express several types of high-threshold Ca^{2+} channels. In pyramidal neurons of neocortex and hippocampus, as well as in mitral cells, expression of L-type and R-type Ca^{2+} channels allows for global Ca^{2+} increases triggered by Na^+ channel dependent dendritic backpropagating action potentials. These Ca^{2+} increases are linked to a number of processes, including dendritic transmitter release and long-term forms of synaptic plasticity. As described in more detail below, Purkinje neurons express P/Q type Ca^{2+} channels in their dendrites that can be activated by climbing fiber synaptic inputs, leading to the generation of complex spikes at the soma (Llinás and Sugimori, 1980).

Dendritic K^+ Conductances

Dendritic excitability is controlled by a number of different types of voltage and Ca^{2+} gated K^+ conductances. One of the best characterized examples is the transient A-type K^+ channel. These conductances are strictly voltage dependent and are rapidly activated by membrane depolarization but inactivate quickly following more sustained depolarization. A-type K^+ channels are strongly and nonuniformly expressed in CA1 hippocampal pyramidal neurons, with an increase in density in more distal dendritic regions. Their kinetics allow them to control the spread of fast dendritic signals such as backpropagating action potentials, while their effectiveness is dramatically reduced following more sustained membrane depolarization (Hoffman et al., 1997).

Many dendrites as well as spines express small conductance K^+ (SK) channels which are solely activated by increases in intracellular Ca^{2+} concentration (Adelman et al., 2012). Because spatiotemporal Ca^{2+} increases in dendrites and spines are tightly regulated by multiple uptake mechanisms, the conditions of SK channel activation are quite complex and not only depend on the density and kinetics of the conductances generating Ca^{2+} influx, but also on the proximity between the sites of Ca^{2+} influx and SK channel expression.

BACKPROPAGATION OF ACTION POTENTIALS INTO DENDRITES

One of the most studied functional properties of active dendrites is the presence of dendritic action potentials. Extracellular field recordings from the hippocampus and intracellular recording from the cell body of a number of neurons had long provided indirect evidence for their existence. However, definitive proof for dendritic action potentials was obtained only by direct intradendritic recordings. One of the earliest demonstrations showing the existence of dendritic spikes came from sharp electrode recordings performed in cerebellar Purkinje cells (Llinás and Sugimori, 1980), which generate fast spikes mediated by Na^+ channels at the soma. By contrast, dendritic recordings revealed the presence of much slower spikes with large amplitudes, mediated by high threshold Ca^{2+} channels (Fig. 17.12). More recently, the use of patch electrodes in combination with microscopy techniques allowing for electrode placement on dendritic processes under visual control has led to a flurry of studies on dendritic function. Collectively, these studies have shown that dendritic action potentials are a common feature in many different types of neurons.

The presence of dendritic action potentials poses an important question: Where do dendritic action potentials *initiate*? A dendritic site of spike initiation would mean that activation of a small number of excitatory synaptic inputs is sufficient to trigger neuronal activity. As a consequence, the ability of a neuron to integrate a large number of excitatory and inhibitory synaptic inputs to generate neuronal output would be severely compromised. Alternatively, even in active dendrites and following dendritic excitatory synaptic inputs, action potentials might still initiate in the soma or axon, before propagating back into the dendritic tree. To directly address this question, the precise timing of action potentials had to be determined by simultaneously recording from both the soma and dendrite of a single neuron. In a landmark study Stuart and Sakmann (1994), visualized whole-cell patch recordings from the soma and apical dendrite of layer 5 pyramidal cells showed that action potentials are detected

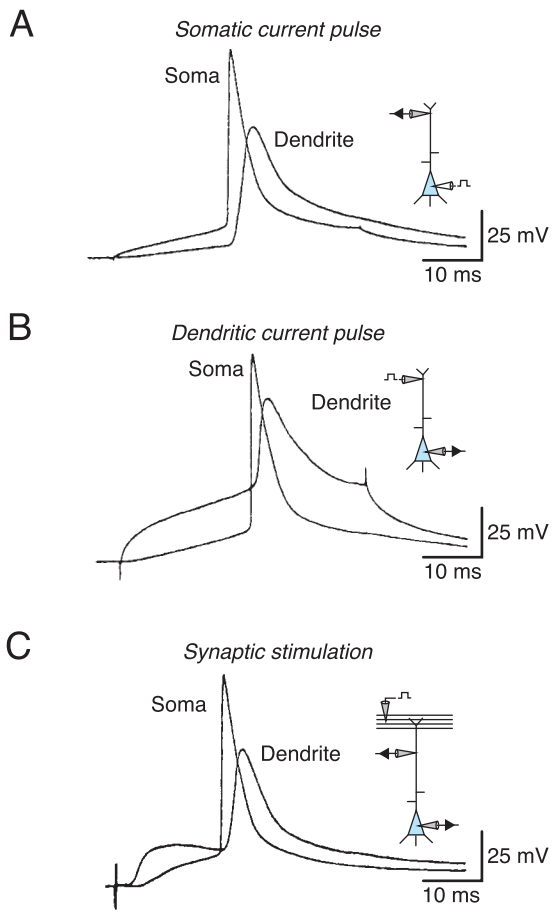

FIGURE 17.13 Direct demonstration of active backpropagation into dendrites using dual-patch recordings from soma and dendrites of a layer 5 pyramidal neuron in a slice preparation of rat neocortex. Depolarizing current injection in either the soma (A) or the dendrite (B) elicits an action potential first in the soma before reaching the dendrite. (C) The same result is obtained with activation of layer I excitatory synaptic inputs to distal dendrites. *From Stuart and Sakmann (1994).*

first in the soma, even following depolarization of the dendritic membrane by current steps applied via the recording electrode or following activation of distally located excitatory synaptic inputs (Fig. 17.13). In later studies, simultaneous recordings from the soma and the axon of different neurons revealed that spike initiation often occurs in the axon (Stuart et al., 1997). The low spike threshold in the axon is likely mediated by several factors, including an extremely high density of Na^+ channels (Kole et al., 2008), a relatively hyperpolarized activation voltage for Na^+ channels, and the extremely small capacitance of the small-diameter axon.

While backpropagating action potentials can be recorded from many neurons, their properties are quite distinct from axonal action potentials. As can be seen in the dendritic recordings obtained from layer 5 pyramidal cells (Fig. 17.13), dendritic action potential amplitudes are often smaller in amplitude compared

to somatic ones, in large part due to a low Na^+ channel density. Thus, in contrast to axonal action potential propagation, which is very robust, due to a high density of Na^+ channels expressed in the axon or at nodes of Ranvier, backpropagating spikes have a comparatively low safety factor. As a consequence, multiple mechanisms can control the spread of backpropagating spikes, such as dendritic K^+ channels (Hoffman et al., 1997), synaptic inhibition (Tsubokawa and Ross, 1996; Xiong and Chen, 2002), or changes in the electrotonic structure at dendritic branch points (Spruston et al., 1995). Similarly, high frequency trains of action potentials that can propagate in the axon without any decrement can experience a strong reduction in amplitude in the dendrite, as an increasing number of Na^+ channels remain in a state of inactivation, thereby progressively reducing the number of available Na^+ channels for each spike in a train (Spruston et al., 1995).

While axonal spike initiation has been well documented for a number of cell types, there are exceptions to this concept. Mitral/tufted cells in the olfactory bulb receive their excitatory synaptic input in the olfactory glomerulus, at the distal end of their primary dendrites. Both experimental data and computer simulations have shown that, for these neurons, strong excitatory input can trigger dendritic spikes which then actively propagate toward the axon, while weaker inputs can lead to spike initiation in the axon, followed by nondecremental backpropagation into the apical dendrite (Chen et al., 1997).

Backpropagating Action Potentials Can Trigger Transmitter Release from Dendrites

Are backpropagating action potentials just a curious epiphenomenon or do they play important functional roles? It is now understood that for many types of neurons the simple distinction between dendrites as recipient elements and axons as the site of sole neuronal output does not hold true. Dendrites can liberate a number of different types of neurotransmitters in a Ca^{2+}-dependent manner, either by means of vesicular release or via more unconventional forms of signaling. Dendritic release can occur at dendrodendritic synapses, which are common in the retina, the thalamus, and the olfactory bulb (Margrie and Urban, 2008). An important and well-studied model system is the olfactory mitral/tufted cell, which is connected to axonless granule cells via dendrodendritic synapses formed by lateral dendrites that often extend over 1 mm in length (Fig. 17.14A,C). Activation of mitral/tufted cells by sensory inputs generates action potentials, which then propagate along the lateral (secondary) dendrites, mediated by dendritic Na^+ channel activation. In turn, this leads to the opening of both low- and high threshold (P/Q-type) Ca^{2+} channels (Fig. 17.14C), generating large Ca^{2+} transients along the entire lateral dendrite (Xiong and Chen, 2002). These dendritic Ca^{2+} increases then trigger the release of glutamate from mitral cell dendrites. Glutamate can bind to AMPA and NMDA receptors expressed on the same mitral cell dendrite, generating a form of autoexcitation (Nicoll and Jahr, 1982). In addition, glutamate release binds to postsynaptic AMPA and NMDA receptors expressed on the large spines of granule cells, triggering Ca^{2+} influx mediated by either NMDA receptor or low-threshold (T-type) Ca^{2+} channels (Chen et al., 2000; Isaacson and Strowbridge, 1998). The resulting Ca^{2+} changes in granule cells can be limited to a single spine (Egger et al., 2005), which in principle could result in GABA release onto the same mitral cell dendrite where glutamate release occurred (Fig. 17.14B). Such self-inhibition of the mitral cell occurs in the wake of the passing backpropagating spike, due to the delay associated with transmitter release at the two synapses. Alternatively, Ca^{2+} increases in granule cells can be global, in which case GABA release can impact the lateral dendrites formed by mitral/tufted cells belonging to a different glomerulus (Fig. 17.14A), generating a form of lateral inhibition (Mori et al., 1999).

It is important to point out that the dendritic release of neurotransmitter is not limited to dendrodendritic synapses, but can also occur from postsynaptic sites adjacent to axodendritic synaptic contacts. Such forms of dendritic release, typically referred to as retrograde signaling, can involve conventional neurotransmitters such as glutamate or GABA, gases such as nitric oxide (NO), peptides, or lipid derivatives such as endocannabinoids, to name a few. What is common to these forms of retrograde signaling is that transmitter release (or—in the case of the endocannabinoids—transmitter synthesis; see Chapter 8) is strongly Ca^{2+} dependent, and that dendritic release, via binding to presynaptic receptors, ultimately influences some aspect of presynaptic transmitter release (Regehr et al., 2009). Ultimately, dendritic release of neurotransmitters is a dynamic process that can range from highly localized release to more global patterns, depending on the spatiotemporal pattern of dendritic Ca^{2+} changes.

Backpropagating Spikes Can Allow for Nonlinear Interactions with Synaptic Inputs

Under physiological conditions, backpropagating action potentials rarely occur in isolation, but during ongoing synaptic activity. How does backpropagation influence postsynaptic integration? For proximal dendritic regions, the activation of dendritic voltage-gated

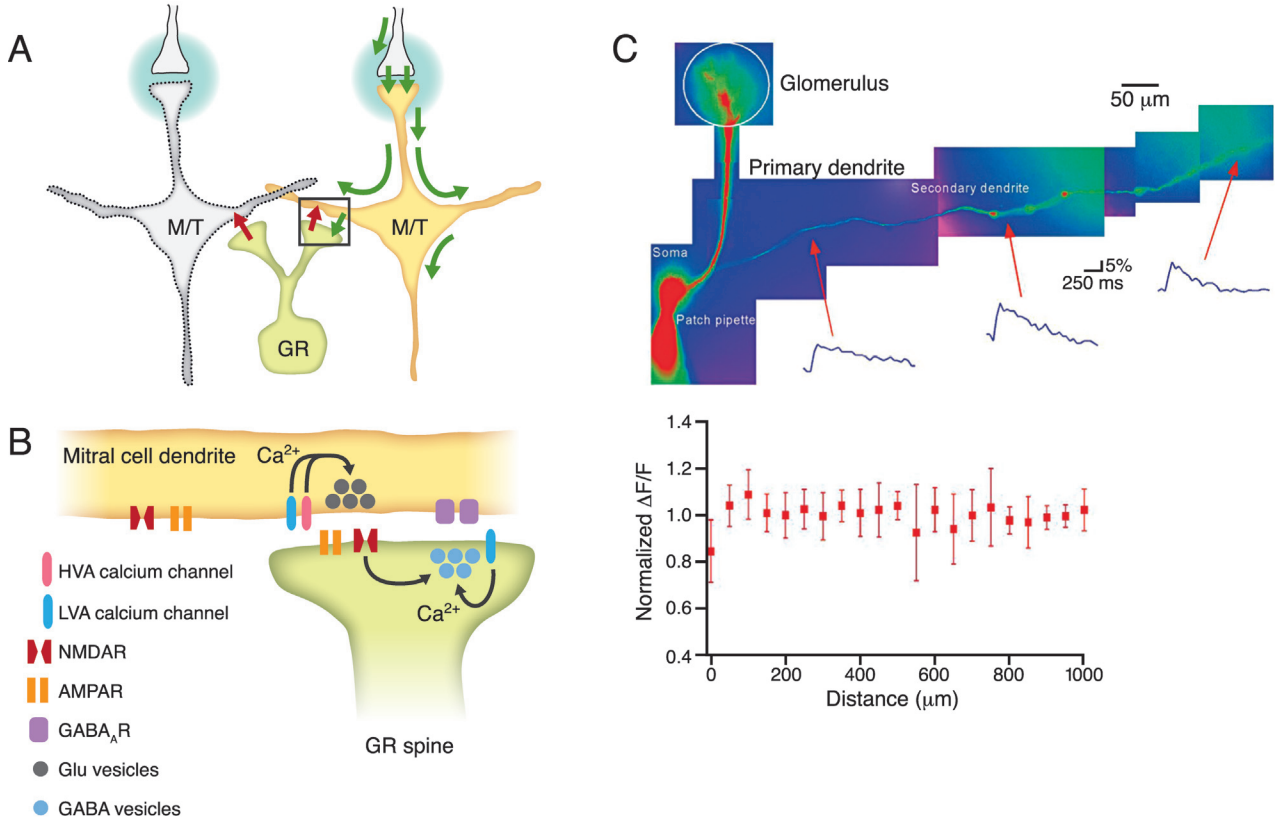

FIGURE 17.14 **Dendrodendritic synaptic signaling in olfactory microcircuits.** (A) Sensory inputs excite M/T cells (short green arrows) inside glomeruli (green circles), triggering active spike propagation through the entire cell (green arrows), resulting in synaptic excitation of granule cells through glutamate release at dendrodendritic synapses (area outlined by black box). The excitation of granule cells leads to the release of GABA (red arrows), mediating recurrent and lateral inhibition of M/T cells. GR: granule cell. *Adapted from Rojas-Libano and Kay (2008).* (B) Close-up of reciprocal dendrodendritic synapse as outlined in (A). Depolarization of a mitral cell dendrite (yellow) evokes release of glutamate, mediated by the opening of either high voltage activated (HVA) or low voltage activated (LVA) Ca^{2+} channels. Glutamate then activates both AMPA and NMDA receptors on granule cell spines (green). In turn, spine limited local Ca^{2+} influx via NMDA receptors or LVA Ca^{2+} channels could trigger the vesicular release of GABA, mediating recurrent inhibition of mitral cells. *Adapted from Urban and Castro (2010).* (C) Action potential propagation in mitral cell secondary dendrites, as detected by Ca^{2+} spike-evoked Ca^{2+} increases. Fluorescence measurements are plotted in the graph below, showing full propagation up to 1000 micrometers. *From Xiong and Chen (2002).*

conductances that accompany backpropagation leads to a significant increase in membrane conductance and a shortening of the membrane time constant. As a consequence, EPSPs and IPSPs will have a significantly shorter waveform and amplitude, which will transiently limit or "reset" synaptic integration.

In more distal dendrites where backpropagation is typically extremely fragile, properly timed excitatory synaptic inputs can generate highly nonlinear and spatially confined amplification of backpropagating signals. In layer 5 pyramidal neurons this amplification is thought to be generated by voltage-gated Na^+ channels (Fig. 17.15), whose activation requires the near-synchronous arrival of an EPSP and a backpropagating spike (Stuart and Hausser, 2001). In CA1 pyramidal neurons, backpropagation under conditions of low synaptic activity is curtailed by the dendritic expression of A-type K^+ conductances, which are open at rest and thereby limit efficient flow of dendritic signals. However, excitatory inputs can lead to the rapid and transient inactivation of these A-type K^+ currents, allowing a properly timed backpropagating action potential to encounter a dendritic region with a smaller leak conductance. Regardless of the exact mechanism, a synaptically controlled amplification of backpropagating responses and the resulting local changes in dendritic Ca^{2+} influx could serve as a mechanism for detecting coincident pre- and postsynaptic firing, and might underlie spike-timing dependent forms of plasticity (Magee and Johnston, 1997).

ACTIVE DENDRITES AMPLIFY SYNAPTIC INPUTS

As mentioned above, in most cases neuronal output is generated by an axonal spike initiation zone. However,

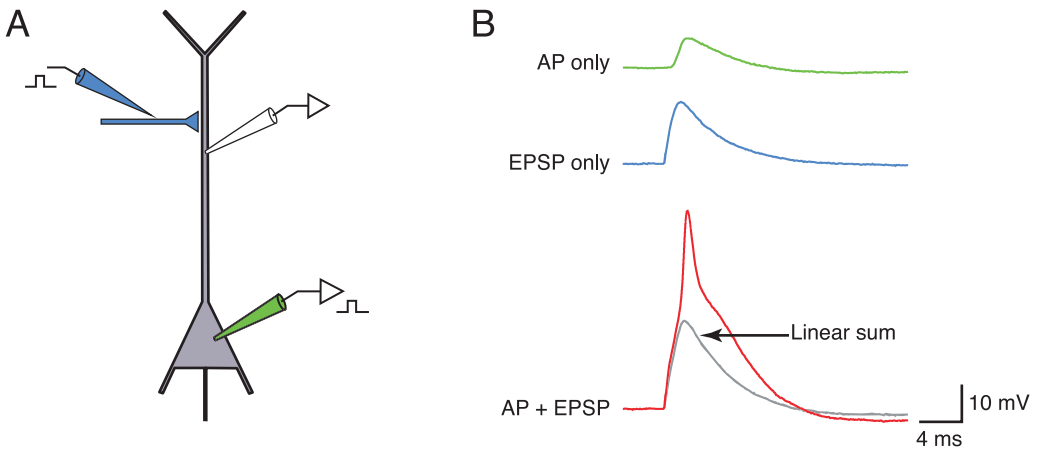

FIGURE 17.15 **Coincidence detection mediated by simultaneous EPSPs and backpropagating action potentials.** (A) Schematic showing recording configuration. Simultaneous somatic (green pipette) and dendritic (white pipette) recordings are obtained from a layer 5 pyramidal neuron and EPSPs are evoked by stimulation of synaptic inputs (blue pipette) near the dendritic recording site. (B) Top trace: backpropagating action potential initiated by somatic current injection, as recorded in the dendrite. Middle trace: EPSP recorded at the same dendritic location. Bottom trace: response evoked by simultaneous generation of backpropagating action potential and EPSP. The linear sum of the action potential and EPSP is also shown for comparison. *Adapted from London and Hausser (2005).*

this does not rule out the generation of *local* dendritic action potentials. Such local events are particularly prominent when dendritic depolarization is mediated by the synchronous activation of excitatory synaptic inputs to a local dendritic region. As we discussed above, dendritic branches often have a large input impedance, such that the synchronous activation of only a small number of synaptic inputs is required to reach threshold for local spike generation. Local spikes therefore form a powerful mechanism to overcome synaptic attenuation. For example, parallel fiber synaptic inputs formed by cerebellar granule cells can trigger local Ca^{2+} spikes in Purkinje cell dendrites (Rancz and Hausser, 2006). In pyramidal cells of neocortex and hippocampus, excitatory synaptic inputs to the distal portion of the apical dendritic trigger local spikes mediated by the activation of either Na^{+} and/or Ca^{2+} channels (Golding and Spruston, 1998, Schiller et al., 1997), while synaptic inputs to basal dendrites can trigger local regenerative events mediated primarily by the activation of NMDA receptors (Schiller et al., 2000). Local dendritic spikes can also be generated if distal dendritic depolarizations have sufficient time to reach threshold for the activation of dendritic Na^{+} and Ca^{2+} channels, prior to spike initiation in the axon where spike threshold is normally lowest. This can occur when depolarization of the soma/axon region is strongly attenuated, for example by properly timed shunting inhibition.

As discussed above, the apical dendrite of mitral cells in the olfactory bulb allows for the propagation of a locally generated dendritic action potential toward the soma and into the axon. However, in the majority of cases, propagation of locally generated spikes towards the soma/axon region is poor (Golding and Spruston, 1998). Due to the low density of voltage gated channels, dendritic action potentials have a low safety factor to begin with. Furthermore, spikes propagating towards the soma encounter branch points at which small diameter branches are connected to a larger diameter parent branch and to a second "sister" branch. As discussed earlier for the spread of EPSPs in passive dendrites, orthodromic current flow in such segments encounters a large conductance load, leading to a progressively smaller depolarization in the parent branch, ultimately leading to spike failure. Thus, the electrotonic structure of a dendritic tree poses strong limits to the effective forward propagation of dendritic action potentials, whereas backpropagation is significantly more robust (see also Fig. 17.8).

How does the presence of synaptically evoked dendritic spikes change the integrative properties of a neuron, for example a pyramidal cell? It is possible that individual dendritic branches and their synaptic inputs function as independent functional units, each of which is able to generate a local spike (Archie and Mel, 2000). Under this scenario, synaptic inputs converging onto a single branch are more effective compared to the same number of active synapses distributed over different branches, since in the latter case no local spikes are generated. However, as outlined above, local spikes generated in a single dendritic branch will typically not trigger an action potential in the soma. For this to occur, multiple dendritic branches would have to generate local spikes in a near simultaneous fashion. In this way, synaptic integration in pyramidal cells can be viewed as a multilayer process, with integration in individual branches forming the first layer, integration of responses

from neighboring branches forming a second layer, and so forth (Hausser and Mel, 2003). While the overall validity of this idea remains to be determined, it is clear that the generation of local spikes enhances the computational complexity of dendritic integration and plasticity. For example, in CA1 pyramidal neurons, the generation of local dendritic spikes evoked by synchronous firing of a small number of synaptic inputs can mediate localized Ca^{2+} increases that trigger long-term synaptic plasticity at the activated synapses, without triggering action potentials in the axon (Golding et al., 2002).

ACTIVE DENDRITES CONTROL NEURONAL OUTPUT

In addition to controlling synaptic integration and backpropagation, the conductances expressed in dendrites have a strong influence on axonal output. This can be illustrated for the unique firing patterns of cerebellar Purkinje cells (Fig. 17.12) which are the target of powerful climbing fiber synapses that contact the proximal dendritic tree. In the absence of synaptic inputs, Purkinje cells generate spontaneous actions potentials mediated by fast Na^+ and delayed K^+ channels expressed in the soma and axon. Continuous firing is mediated by persistent Na^+ channels that generate a so-called pacemaker current. Due to the low expression of Na^+ channels in Purkinje cell dendrites, axonal spikes do not propagate into the dendritic tree. Therefore, P-type Ca^{2+} channels expressed in the dendritic tree are not activated under these conditions. Following the activation of climbing fiber inputs, a large postsynaptic EPSP is generated in the proximal dendritic tree, in turn triggering a Ca^{2+} spike and widespread Ca^{2+} influx. This results in the activation of BK channels which are both voltage and Ca^{2+} dependent, leading to the hyperpolarization of the dendritic membrane and the termination of the Ca^{2+} spike. Because of the slow kinetics of the dendritically generated depolarizing and hyperpolarizing responses, their relative proximity to the soma/axon region, and the large diameter of Purkinje cell dendrites, they easily propagate toward the soma where they can effectively modulate neuronal output. Thus, the slow Ca^{2+} spike depolarizes the soma/axon region, leading to a burst of Na^+ dependent action potentials, termed the complex spike, while the subsequent hyperpolarization leads to a pause in neuronal output.

From this example it is apparent that complex firing patterns can be generated by the separation of fast and slow conductances into distinct neuronal compartments, a scenario which applies to a number of other cell types, including layer 5 pyramidal cells. Studies have shown that in these neurons strong synaptic input to the distal dendrites can generate a local Ca^{2+} spike which generates sufficient depolarization in the axon to generate burst firing (Schiller et al., 1997). Interestingly, the threshold for the generation of dendritic Ca^{2+} spikes can be significantly reduced by a properly timed backpropagating action potential that coincides with the distal dendritic input (Larkum et al., 1999), suggesting that effective coupling between axonal and dendritic compartment is bidirectional in pyramidal cells. As outlined above, this is in marked contrast to Purkinje neurons, where the generation of Ca^{2+} spikes by climbing fiber inputs is all-or-none and not influenced by backpropagating action potentials, due to the lack of dendritic Na^+ channels.

A detailed understanding of the dynamic interplay of different types of conductances expressed in separate neuronal compartments is greatly aided by the use of computer simulations. For example, a two-compartment model with a soma/axon segment containing fast voltage-gated Na^+ and K^+ channels and a dendritic segment with slower Ca^{2+} channels and two types of K^+ channels (Fig. 17.16) can generate a number of different neuronal output patterns (Pinsky and Rinzel, 1994). Careful simulations with this model have revealed that neuronal output is determined by the relative size of the dendritic tree relative to the soma, as well as by the effective linkage between soma/axon and dendritic region, which in the model can be simulated by changing the value of the coupling conductance linking the two compartments (Fig. 17.16A). For scenarios in which dendrites are short and coupling is strong, the model reduces to a single compartment and generates tonic Na^+ dependent action potentials. However, for larger dendritic compartments and less effective coupling, the model will generate rhythmic bursts of action potentials (Fig. 17.16B). Thus, both dendritic morphology as well as their active properties are important in determining neuronal output (Mainen and Sejnowski, 1996).

Ca^{2+} SIGNALING IN DENDRITIC SPINES

Dendritic spines are a fundamental feature of many different types of neurons and are the site of excitatory synapses. Their unique structure has long fascinated anatomists and physiologists alike, but their small size has made them virtually inaccessible to direct electrophysiological recordings. We now know that both synaptic inputs and backpropagating action potentials can trigger Ca^{2+} increases within spines, mediated by the activation of ligand-gated receptors such as NMDA receptors and Ca^{2+} permeable AMPA receptors, voltage-gated Ca^{2+} channels, and release of Ca^{2+} from internal stores. As discussed elsewhere

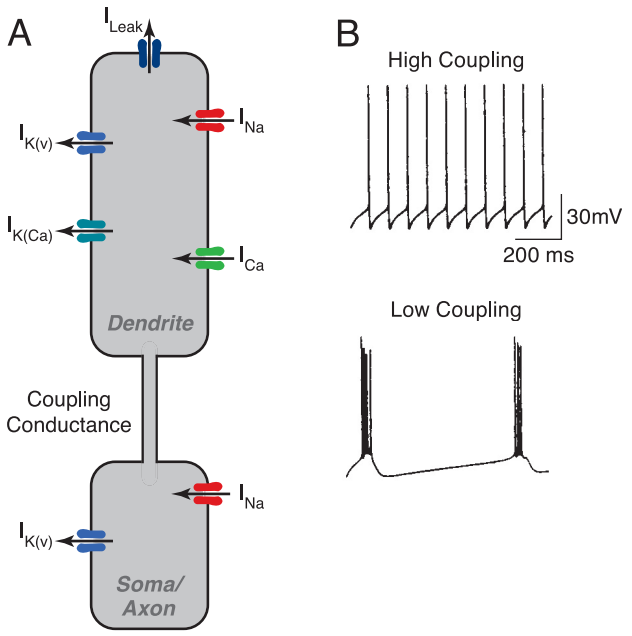

FIGURE 17.16 Dendritic conductances shape spike output in the soma/axon region. (A) Schematic of a two-compartment model neuron (Pinsky and Rinzel, 1994). The larger compartment represents all the dendrites lumped together, and the smaller compartment represents the soma and the initial segment of the axon. The two compartments are coupled by a variable electrical conductance, and each has a different complement of ion channels. *Adapted from Connors and Regehr (1996).* (B) Examples of axonal firing patterns simulated in two-compartment model, generated by changes of the electrical conductance linking dendritic and soma/axon compartment.

(Chapters 4, 18 and 20), Ca^{2+} increases are thought to be essential for a number of signaling cascades leading to changes in dendritic excitability, spine morphology, and synaptic plasticity. Many of these processes are limited to individual synapses and therefore need to remain highly localized, suggesting that the initial trigger (i.e., Ca^{2+} influx) is limited to individual spines. The development of powerful light microscopical methods with exquisite temporal and spatial resolution such as multiphoton microscopy has made it possible to directly test this idea (Fig. 17.17).

Based on the electrotonic structure of the spine, voltage changes in the parent dendrite should readily invade the spine head (Box 17.2). In support of this, experiments have shown that in pyramidal neurons backpropagating action potentials lead to Ca^{2+} influx in both spines and adjacent dendritic branches. Notably, Ca^{2+} changes in the spine occur simultaneously to the ones in the parent dendrite, indicating that spines themselves are the site of Ca^{2+} influx (Fig. 17.17B). Pharmacological experiments show that for many types of neurons, spine Ca^{2+} influx evoked by backpropagating action potentials is mediated by voltage-gated Ca^{2+} channels. The size of the spine compartment predicts that the number of Ca^{2+} channels mediating Ca^{2+} influx is very small. Indeed, trial-by-trial measurements reveal a much higher variability of Ca^{2+} changes in spines compared to dendrites (Fig. 17.17C), also indicating that the probability of Ca^{2+} channel opening is low.

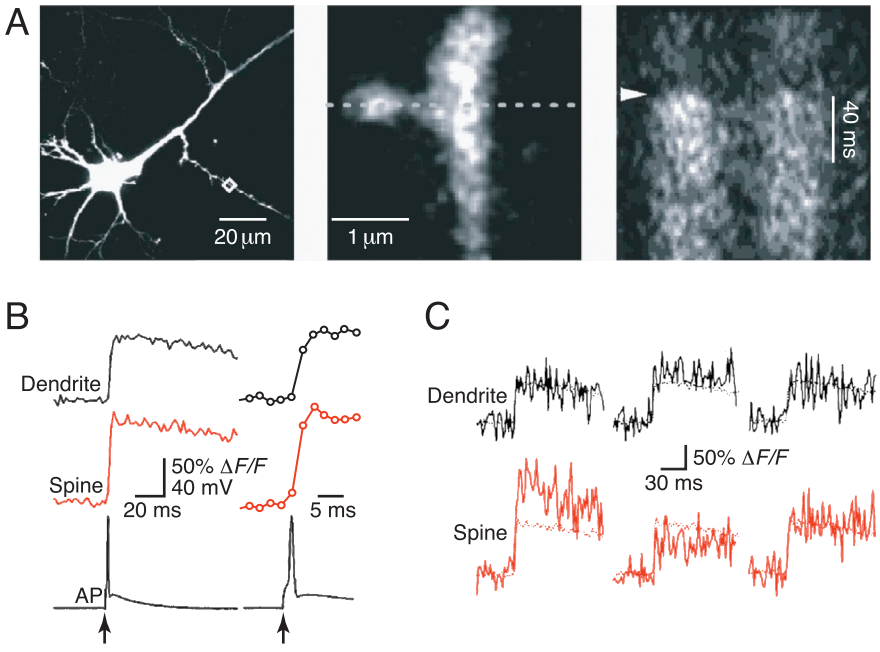

FIGURE 17.17 Ca^{2+} signaling in dendrites and spines. (A) Left: Image of CA1 pyramidal cell loaded with the Ca^{2+} -sensitive dye Fluo-4. Middle: Close-up of individual spine and parent dendritic branch outlined by box in left image. Dashed line indicates location of line scan. Right: Line scan over spine and adjacent dendritic branch shows increases in intradendritic and intra-spine Ca^{2+} following backpropagating action potential. Time of somatic spike is marked by arrow. (B) Average responses showing spike-evoked increases in Ca^{2+} in the dendrite and larger increases in the spine. Traces on right show responses on faster time scale. (C) Ca^{2+} increases measured in individual trials show low fluctuations in dendrites but higher fluctuations in spines, indicating that spine Ca^{2+} signals are mediated by opening of a small number of voltage-gated Ca^{2+} channels. *From Sabatini and Svoboda (2000).*

How do individual synaptic inputs control Ca^{2+} influx in spines? As outlined earlier in this chapter, theoretical models have long predicted that the spine voltage signal generated by an excitatory synapse contacting a spine head must be significantly larger than the response measured in the parent dendrite (Fig. 17.11; see also Box 17.2). Thus, glutamate release from a single release site contacting an individual spine might generate sufficient depolarization to trigger Ca^{2+} influx. To test this idea experimentally has long been a challenge since few preparations allow for the activation of individual synaptic inputs onto a well-isolated spine. Furthermore, the use of pharmacological blockers for Ca^{2+} channels also interferes with synaptic release of glutamate, making it difficult to isolate the postsynaptic sources of synaptically induced Ca^{2+} changes. These problems can be overcome by the use of multiphoton laser photoactivation, which allows for the liberation of "caged" compounds with high spatial resolution. In this way glutamate, which in its caged form has no biological activity, can be photo-liberated near a spine under study, thereby mimicking a glutamate transient associated with synaptic release from an individual terminal (Carter and Sabatini, 2004). Such experiments have shown that "synaptically" activated spine Ca^{2+} increases can differ substantially from the ones evoked by backpropagating spikes. For example, in medium spiny neurons of the striatum, synaptic inputs trigger highly localized Ca^{2+} changes in spines, which are mediated by NMDA and Ca^{2+} permeable AMPA receptors (Fig. 17.18). Similar findings using the same techniques have been made for other neuronal types, confirming that synaptically evoked Ca^{2+} transients are often limited to the stimulated spine (Bloodgood and Sabatini, 2007a).

Given their small size and their electrical and biochemical isolation from the parent dendrite, it is tempting to conclude that spines form the most basic computational unit of a dendritic tree. However, such a statement might be premature. In hippocampal pyramidal neurons, individual spines express SK conductances, which are activated by Ca^{2+} increases evoked by individual synaptic inputs. While spine Ca^{2+} increases can be generated by activation of NMDA receptors, it is only the Ca^{2+} increase mediated by R-type Ca^{2+} channel opening that is responsible for SK opening (Bloodgood and Sabatini, 2007b). The activation of SK channels by Ca^{2+} increases evoked specifically by R-type Ca^{2+} channel opening—and not by NMDA receptor activation—indicates that, despite their small size, individual spines can generate distinct Ca^{2+} signals (so-called Ca^{2+} microdomains), which can trigger distinct signaling cascades.

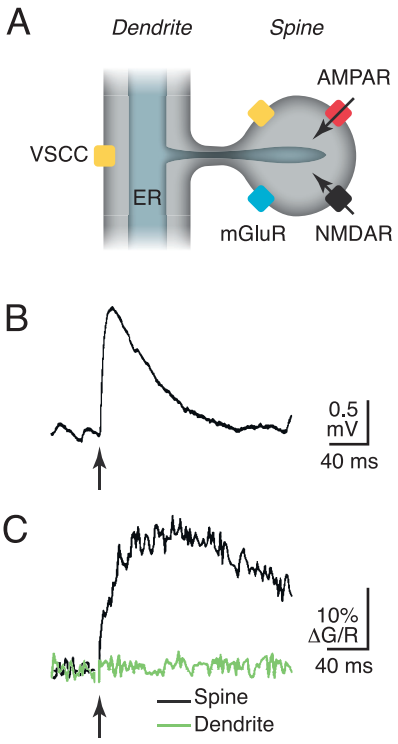

FIGURE 17.18 Synaptically evoked Ca^{2+} signals in individual spines. (A) Schematic indicating potential sources of spine Ca^{2+} increases in medium spiny neurons of the striatum, including Ca^{2+} permeable AMPA and NMDA receptors, voltage-gated Ca^{2+} channels and Ca^{2+} release from the endoplasmic reticulum. (B) Somatic depolarization evoked by brief glutamate transients limited to individual spines using multiphoton laser uncaging of glutamate. (C) For the same glutamate transient, Ca^{2+} increases measured as fluorescent transients can be detected in spine (black trace) but not in parent dendrite (green trace) and are mediated by Ca^{2+} influx through AMPA and NMDA receptors. *Adapted from Carter & Sabatini (2008).*

CONCLUSION

Dendrites show incredible diversity in morphology, electrotonic structure and in the types, properties, and distributions of voltage- and Ca^{2+} gated ion channels expressed in their membrane. This diversity and the variety of phenomena it generates can be equally exciting and overwhelming. Nevertheless, a number of general principles are starting to emerge. For example, the generation of local dendritic spikes or backpropagating action potential is a feature common to almost all types of neurons under study. As discussed in this chapter, dendritic spikes can be involved in the release of neurotransmitters, in the detection of simultaneous pre- and postsynaptic firing, the boosting of synchronously active synaptic inputs arriving on a single branch, and the generation of highly complex neuronal firing patterns. The challenge for future studies will be to causally link these cellular functions to computations on a behavioral level.

Note: Parts of this chapter have been adapted from Chapters 5 and 17 by Byrne and Shepherd in the previous edition of this book.

References

Adelman, J.P., Maylie, J., Sah, P., 2012. Small-conductance Ca^{2+}-activated K^+ channels: form and function. Annu. Rev. Physiol. 74, 245–269.

Agmon-Snir, H., Carr, C.E., Rinzel, J., 1998. The role of dendrites in auditory coincidence detection. Nature. 393, 268–272.

Alvarez, V.A., Sabatini, B.L., 2007. Anatomical and physiological plasticity of dendritic spines. Annu. Rev. Neurosci. 30, 79–97.

Araya, R., Eisenthal, K.B., Yuste, R., 2006. Dendritic spines linearize the summation of excitatory potentials. Proc. Natl. Acad. Sci. U.S. A. 103, 18799–18804.

Archie, K.A., Mel, B.W., 2000. A model for intradendritic computation of binocular disparity. Nat. Neurosci. 3, 54–63.

Bloodgood, B.L., Sabatini, B.L., 2007a. Ca^{2+} signaling in dendritic spines. Curr. Opin. Neurobiol. 17, 345–351.

Bloodgood, B.L., Sabatini, B.L., 2007b. Nonlinear regulation of unitary synaptic signals by CaV(2.3) voltage-sensitive calcium channels located in dendritic spines. Neuron. 53, 249–260.

Carnevale, N.T., Tsai, K.Y., Claiborne, B.J., et al., 1997. Comparative electrotonic analysis of three classes of rat hippocampal neurons. J. Neurophysiol. 78, 703–720.

Carter, A., Sabatini, B., 2008. Spine calcium signaling. In: Stuart, G., Spruston, N., Hausser, M. (Eds.), Dendrites. Oxford University Press, Oxford.

Carter, A.G., Sabatini, B.L., 2004. State-dependent calcium signaling in dendritic spines of striatal medium spiny neurons. Neuron. 44, 483–493.

Chen, W.R., Midtgaard, J., Shepherd, G.M., 1997. Forward and backward propagation of dendritic impulses and their synaptic control in mitral cells. Science. 278, 463–467.

Chen, W.R., Xiong, W., Shepherd, G.M., 2000. Analysis of relations between NMDA receptors and GABA release at olfactory bulb reciprocal synapses. Neuron. 25, 625–633.

Connors, B.W., Regehr, W.G., 1996. Neuronal firing: does function follow form? Curr. Biol. 6, 1560–1562.

Davie, J.T., Kole, M.H., Letzkus, J.J., et al., 2006. Dendritic patch-clamp recording. Nat. Protoc. 1, 1235–1247.

Denk, W., Svoboda, K., 1997. Photon upmanship: why multiphoton imaging is more than a gimmick. Neuron. 18, 351–357.

Egger, V., Svoboda, K., Mainen, Z.F., 2005. Dendrodendritic synaptic signals in olfactory bulb granule cells: local spine boost and global low-threshold spike. J. Neurosci. 25, 3521–3530.

Gillessen, T., Alzheimer, C., 1997. Amplification of EPSPs by low Ni^{2+}- amiloride-sensitive Ca^{2+} channels in apical dendrites of rat CA1 pyramidal neurons. J. Neurophysiol. 77, 1639–1643.

Golding, N.L., Spruston, N., 1998. Dendritic sodium spikes are variable triggers of axonal action potentials in hippocampal CA1 pyramidal neurons. Neuron. 21, 1189–1200.

Golding, N.L., Staff, N.P., Spruston, N., 2002. Dendritic spikes as a mechanism for cooperative long-term potentiation. Nature. 418, 326–331.

Hausser, M., Mel, B., 2003. Dendrites: bug or feature? Curr. Opin. Neurobiol. 13, 372–383.

Hoffman, D.A., Magee, J.C., Colbert, C.M., et al., 1997. K^+ channel regulation of signal propagation in dendrites of hippocampal pyramidal neurons. Nature. 387, 869–875.

Isaacson, J.S., Strowbridge, B.W., 1998. Olfactory reciprocal synapses: dendritic signaling in the CNS. Neuron. 20, 749–761.

Jack, J.J.B., Noble, D., Tsien, R.W., 1975. Electric current flow in excitable cells. Clarendon Press, Oxford.

Kole, M.H., Ilschner, S.U., Kampa, B.M., et al., 2008. Action potential generation requires a high sodium channel density in the axon initial segment. Nat. Neurosci. 11, 178–186.

Larkum, M.E., Zhu, J.J., Sakmann, B., 1999. A new cellular mechanism for coupling inputs arriving at different cortical layers. Nature. 398, 338–341.

Llinás, R., Sugimori, M., 1980. Electrophysiological properties of in vitro Purkinje cell dendrites in mammalian cerebellar slices. J. Physiol. 305, 197–213.

London, M., Hausser, M., 2005. Dendritic computation. Annu. Rev. Neurosci. 28, 503–532.

Magee, J.C., 2000. Dendritic integration of excitatory synaptic input. Nat. Rev. Neurosci. 1, 181–190.

Magee, J.C., Johnston, D., 1997. A synaptically controlled, associative signal for Hebbian plasticity in hippocampal neurons. Science. 275, 209–213.

Mainen, Z.F., Sejnowski, T.J., 1996. Influence of dendritic structure on firing pattern in model neocortical neurons. Nature. 382, 363–366.

Mel, B.W., 1994. Information processing in dendritic trees. Neural. Comput. 6, 1031–1085.

Mel, B.W., Schiller, J., 2004. On the fight between excitation and inhibition: location is everything. Sci. STKE. 2004, PE44.

Mori, K., Nagao, H., Yoshihara, Y., 1999. The olfactory bulb: coding and processing of odor molecule information. Science. 286, 711–715.

Nicoll, R.A., Jahr, C.E., 1982. Self-excitation of olfactory bulb neurones. Nature. 296, 441–444.

Oviedo, H., Reyes, A.D., 2002. Boosting of neuronal firing evoked with asynchronous and synchronous inputs to the dendrite. Nat. Neurosci. 5, 261–266.

Pinsky, P.F., Rinzel, J., 1994. Intrinsic and network rhythmogenesis in a reduced Traub model for CA3 neurons. J. Comput. Neurosci. 1, 39–60.

Rall, W., 1964. Theoretical significance of dendritic trees for neuronal input-output relations. In: Reiss, R.F. (Ed.), Neural Theory and Modelling. Stanford Univ. Press, Stanford, CA.

Rall, W., 1967. Distinguishing theoretical synaptic potentials computed for different soma-dendritic distributions of synaptic input. J. Neurophysiol. 30, 1138–1168.

Rall, W., 1977. Core conductor theory and cable properties of neurons. The Nervous System, Cellular Biology of Neurons. Am. Physiol. Soc.. E. R. Kandel, Bethesda, MD.

Rall, W., Shepherd, G.M., 1968. Theoretical reconstruction of field potentials and dendrodendritic synaptic interactions in olfactory bulb. J. Neurophysiol. 31, 884–915.

Rall, W., Segev, I., Rinzel, J., et al., 1995. The theoretical foundation of dendritic function: selected papers of Wilfrid Rall with commentaries. MIT Press, Cambridge, Mass.

Rancz, E.A., Hausser, M., 2006. Dendritic calcium spikes are tunable triggers of cannabinoid release and short-term synaptic plasticity in cerebellar Purkinje neurons. J. Neurosci. 26, 5428–5437.

Regehr, W.G., Carey, M.R., Best, A.R., 2009. Activity-dependent regulation of synapses by retrograde messengers. Neuron. 63, 154–170.

Rojas-Libano, D., Kay, L.M., 2008. Olfactory system gamma oscillations: the physiological dissection of a cognitive neural system. Cogn. Neurodyn. 2, 179–194.

Sabatini, B.L., Svoboda, K., 2000. Analysis of calcium channels in single spines using optical fluctuation analysis. Nature. 408, 589–593.

Schiller, J., Schiller, Y., Stuart, G., et al., 1997. Calcium action potentials restricted to distal apical dendrites of rat neocortical pyramidal neurons. J. Physiol. 505 (Pt 3), 605–616.

Schiller, J., Major, G., Koester, H.J., et al., 2000. NMDA spikes in basal dendrites of cortical pyramidal neurons. Nature. 404, 285–289.

Shepherd, G.M., 1996. The dendritic spine: a multifunctional integrative unit. J. Neurophysiol. 75, 2197–2210.

Spruston, N., 2008. Pyramidal neurons: dendritic structure and synaptic integration. Nat. Rev. Neurosci. 9, 206–221.

Shepherd, G.M., Koch, C., 1990. Dendritic electrotonus and synaptic integration. In: Shepherd, G.M. (Ed.), The Synaptic Organization of the Brain, third Ed. Oxford Univ. Press, New York, pp. 439–574.

Spruston, N., Schiller, Y., Stuart, G., et al., 1995. Activity-dependent action potential invasion and calcium influx into hippocampal CA1 dendrites. Science. 268, 297–300.

Stuart, G., Sakmann, B., 1995. Amplification of EPSPs by axosomatic sodium channels in neocortical pyramidal neurons. Neuron. 15, 1065–1076.

Stuart, G., Spruston, N., Sakmann, et al., 1997. Action potential initiation and backpropagation in neurons of the mammalian CNS. Trends Neurosci. 20, 125–131.

Stuart, G., Spruston, N., Hausser, M., 2007. Dendrites. Oxford University Press, Oxford; New York.

Stuart, G.J., Hausser, M., 2001. Dendritic coincidence detection of EPSPs and action potentials. Nat. Neurosci. 4, 63–71.

Stuart, G.J., Sakmann, B., 1994. Active propagation of somatic action potentials into neocortical pyramidal cell dendrites. Nature. 367, 69–72.

Tsubokawa, H., Ross, W.N., 1996. IPSPs modulate spike backpropagation and associated $Ca^{2+}i$ changes in the dendrites of hippocampal CA1 pyramidal neurons. J. Neurophysiol. 76, 2896–2906.

Urban, N.N., Castro, J.B., 2010. Functional polarity in neurons: what can we learn from studying an exception? Curr. Opin. Neurobiol. 20, 538–542.

Xiong, W., Chen, W.R., 2002. Dynamic gating of spike propagation in the mitral cell lateral dendrites. Neuron. 34, 115–126.

Zador, A.M., Agmon-Snir, H., Segev, I., 1995. The morphoelectrotonic transform: a graphical approach to dendritic function. J. Neurosci. 15, 1669–1682.